


# Space-time-resolved quantum electrodynamics description of Compton scattering

Scott Glasgow\*

*Mathematics Department, Brigham Young University, Provo, Utah 84602, USA*

Michael J. Ware<sup>†</sup>

*Department of Physics and Astronomy, Brigham Young University, Provo, Utah 84602, USA*

 (Received 16 December 2019; revised 29 October 2020; accepted 4 November 2020; published 3 December 2020)

The standard method for approaching quantum electrodynamic (QED) field theory uses a perturbative  $S$ -matrix approach. This approach is explicitly nondynamical and provides only a one-time, static map between an initial state to be evolved by the “full propagator” of a bona-fide interacting field theory and an asymptotically equivalent effective initial state to be evolved by the “free propagator” of the corresponding noninteracting field theory. We provide a detailed derivation of a nonperturbative and dynamical approach to QED that allows one to study the space-time dynamics of electron-photon interactions directly. As an example of this method, we compute the time-resolved dynamics of Compton scattering for a system with a nontrivial spatial structure in only one dimension while restricting to the case of a single electron and at most one photon. This approach retains the massless photon of quantum electrodynamics in contrast to previous approaches that resorted to using massive bosons [T. Cheng, E. R. Gospodarczyk, Q. Su, and R. Grobe, *Ann. Phys.* **325**, 265 (2010)] to represent the photon. The dynamics of Compton scattering are illustrated using joint probability distributions that evolve in time. This information is compared to that provided by the  $S$  matrix.

DOI: [10.1103/PhysRevA.102.062203](https://doi.org/10.1103/PhysRevA.102.062203)

## I. INTRODUCTION

Quantum electrodynamics (QED) successfully models the fundamental interactions between photons and electrons. These interactions are often studied using the perturbative  $S$ -matrix approach [1–3], typically depicted using Feynman diagrams. This approach is very successful in calculating time-independent quantities such as energies of atomic sub-levels and scattering cross sections. However, it provides only indirect insight into the time-dependent dynamics of the interaction, arguably even for the subset of initial states for the full, interacting-field evolution that nevertheless eventually leads to asymptotically free evolution.

Computing the space-time-resolved dynamics of a fully second-quantized scattering process currently appears intractable for three-dimensional QED, especially for high-intensity radiation fields. However, under the approximation of semiclassical optical fields, Krebs *et al.* have modeled three-dimensional (3D) Compton scattering for intense x-ray photons [4] and compared their theoretical results with experimental measurements made by Fuchs *et al.* [5]. The success of this type of hybrid quantum-classical model derives from deliberately accounting for time-resolved quantum field theory, as championed by Grobe *et al.* [6], and requires a nontrivial process to transition from a quantum field description to a classical field description. An important result of this transition is removing the unphysical self-repulsion of charged

particles via the Coulomb, action-at-a-distance mechanism, which is often present in classical approximations to quantum field theory.

The group of Grobe *et al.* have made great strides in qualitatively visualizing time-resolved particle dynamics in QED-like systems [7–10]. For example, Wagner *et al.* from this group looked at the time evolution of a one-dimensional simplified Hamiltonian based on a Yukawa interaction [10]. This model uses a massive boson as an analog to the photon, and it neglects spin and polarization. They used this simpler interaction in place of the full Dirac-Maxwell QED Hamiltonian to make numerical simulation in one spatial dimension accessible. They produced animations of a bare fermion being dressed by a boson field as well as scattering processes analogous to Compton scattering. We build upon this previous work in developing our description.

Our description is generated by projecting three-dimensional QED onto a single spatial dimension plus time. This projection is accomplished by quantizing in a finite box laterally while allowing infinite expanse in the longitudinal direction. This results in discrete labels for lateral modes and continuous labels for longitudinal modes. This combination allows for essentially one-dimensional calculations, while retaining three-dimensional notions of structure such as polarization and spin. This projection of full QED allows the force mediator to be identified with the massless photon and the fermion to be identified with the (bare) electron. As a projection of full QED, the photon’s coupling-free dispersion relation is that of a relativistic massless particle,

$$E_\gamma = \hbar\omega_\gamma = c\hbar k. \quad (1)$$

\*glasgow@mathematics.byu.edu

†ware@byu.edu

The electron's coupling-free dispersion relation is that of a relativistic massive particle,

$$E_e = \hbar\omega_e = \sqrt{(m_e c^2)^2 + (c\hbar k)^2}, \quad (2)$$

where  $m_e$  is the mass of an electron and  $\hbar k$  is the electron's momentum.

In an earlier article [11] we described this projection process in a manner where the dimensional reduction was accomplished using an analysis of units. In this article, we provide a more robust derivation wherein the discrete lateral quantization process gives rise to an explicit connection between the quantization length and the strength of the electron-photon interaction. To allow computational tractability, we restrict our attention to the lowest lateral mode wherein there is no lateral variation of the wave functions. This results in something like a plane-wave approximation in that all nontrivial dynamics occur in a single dimension. However, it differs from a true plane-wave description in that the lateral dimension is taken as finite so that the electron has a finite probability of being found in a given spatial volume.

We illustrate how this description can be used to calculate the dynamics of Compton scattering in such a one-dimensional system. We compare these computational results to the standard  $S$ -matrix approach and find that the information provided by the  $S$ -matrix is useful but incomplete and is at least as numerically expensive to extract as the full gamut of information that the time-resolved dynamics immediately gives.

## II. DERIVATION

The dynamical form of QED derives from the abstract Schrödinger equation

$$i\hbar \frac{\partial}{\partial t} |\Psi(t)\rangle = H_{\text{QED}} |\Psi(t)\rangle, \quad (3)$$

where the Hamiltonian  $H_{\text{QED}}$  describes the second-quantized interaction of radiation and matter. Following Cohen-Tannoudji [12] *et al.*, we have

$$H_{\text{QED}} = H_D + H_C + H_R + H_I, \quad (4)$$

where the Dirac term  $H_D$  gives the bare energy of electrons and positrons, the Coulomb term  $H_C$  gives the energy associated with charged particles repelling and attracting one another, the radiation term  $H_R$  gives the energy operator for photons, and the interaction term  $H_I$  describes the interaction of matter and radiation. We use this canonical operator to

study the scattering of a photon from an electron, within several approximations. Formally, the terms can be written as

$$\begin{aligned} H_D &= \int d^3\mathbf{r} \Psi^\dagger(\mathbf{r}) [\beta m c^2 - i\hbar c \boldsymbol{\alpha} \cdot \nabla] \Psi(\mathbf{r}), \\ H_C &= \int d^3\mathbf{r} \int d^3\mathbf{r}' \frac{\rho(\mathbf{r})\rho(\mathbf{r}')}{8\pi\epsilon_0 \|\mathbf{r} - \mathbf{r}'\|}, \\ H_R &= \int d^3\mathbf{k} \hbar\omega_{\mathbf{k}} [a_1^\dagger(\mathbf{k})a_1(\mathbf{k}) + a_2^\dagger(\mathbf{k})a_2(\mathbf{k})], \\ H_I &= -qc \int d^3\mathbf{r} \Psi^\dagger(\mathbf{r}) [\boldsymbol{\alpha} \cdot \mathbf{A}_\perp(\mathbf{r})] \Psi(\mathbf{r}). \end{aligned} \quad (5)$$

We discuss each of these terms below, starting with the Dirac term.

The Dirac term  $H_D$  is most easily described in momentum space. The standard Fourier transformation is given by

$$\begin{aligned} \Psi(\mathbf{r}) &= \frac{1}{(2\pi)^{3/2}} \int d^3\mathbf{k} \tilde{\Psi}(\mathbf{k}) e^{i\mathbf{k}\cdot\mathbf{r}}, \\ \tilde{\Psi}(\mathbf{k}) &= \frac{1}{(2\pi)^{3/2}} \int d^3\mathbf{r} \Psi(\mathbf{r}) e^{-i\mathbf{k}\cdot\mathbf{r}}, \end{aligned} \quad (6)$$

where the field  $\Psi$  is a four-component column vector. In momentum space, the Dirac term becomes

$$H_D = \int d^3\mathbf{k} \tilde{\Psi}^\dagger(\mathbf{k}) [\beta m c^2 + \hbar c \boldsymbol{\alpha} \cdot \mathbf{k}] \tilde{\Psi}(\mathbf{k}). \quad (7)$$

The matrix  $\beta$  is defined by

$$\beta = \begin{bmatrix} 1_{2\times 2} & 0_{2\times 2} \\ 0_{2\times 2} & -1_{2\times 2} \end{bmatrix}, \quad (8)$$

and  $\boldsymbol{\alpha}$  is a vector of  $4 \times 4$  matrices with components

$$\begin{aligned} \alpha_1 &= \begin{bmatrix} 0_{2\times 2} & \sigma_x \\ \sigma_x & 0_{2\times 2} \end{bmatrix}, \\ \alpha_2 &= \begin{bmatrix} 0_{2\times 2} & \sigma_y \\ \sigma_y & 0_{2\times 2} \end{bmatrix}, \\ \alpha_3 &= \begin{bmatrix} 0_{2\times 2} & \sigma_z \\ \sigma_z & 0_{2\times 2} \end{bmatrix}, \end{aligned} \quad (9)$$

and

$$\sigma_x = \begin{bmatrix} 0 & 1 \\ 1 & 0 \end{bmatrix}, \quad \sigma_y = \begin{bmatrix} 0 & -i \\ i & 0 \end{bmatrix}, \quad \sigma_z = \begin{bmatrix} 1 & 0 \\ 0 & -1 \end{bmatrix}. \quad (10)$$

With these definitions, the bracketed term in Eq. (7) can be explicitly written as

$$\beta m c^2 + \hbar c \boldsymbol{\alpha} \cdot \mathbf{k} = \begin{bmatrix} m c^2 & 0 & \hbar c k_3 & \hbar c(k_1 - i k_2) \\ 0 & m c^2 & \hbar c(k_1 + i k_2) & -\hbar c k_3 \\ \hbar c k_3 & \hbar c(k_1 - i k_2) & -m c^2 & 0 \\ \hbar c(k_1 + i k_2) & -\hbar c k_3 & 0 & -m c^2 \end{bmatrix}. \quad (11)$$

We can express the matrix (11) as a unitary transformation of the diagonal matrix  $\beta$  as follows:

$$\beta m c^2 + \hbar c \boldsymbol{\alpha} \cdot \mathbf{k} = \mathcal{E}(\mathbf{k}) U(\mathbf{k}) \beta U^\dagger(\mathbf{k}), \quad (12)$$

where

$$\mathcal{E}(\mathbf{k}) = \sqrt{(m c^2)^2 + (\hbar c \mathbf{k})^2}, \quad (13)$$

$$U(\mathbf{k}) = \cos(\theta_{\mathbf{k}}/2) I - \sin(\theta_{\mathbf{k}}/2) \beta \boldsymbol{\alpha} \cdot \hat{\mathbf{k}}, \quad (14)$$

$I$  is the identity matrix, and

$$\theta_{\mathbf{k}} = \arctan\left(\frac{\hbar\|\mathbf{k}\|}{mc}\right), \quad \hat{\mathbf{k}} = \frac{\mathbf{k}}{\|\mathbf{k}\|}. \quad (15)$$

Using this unitary transform, we can rewrite  $H_D$  as

$$H_D = \int d^3\mathbf{k} \mathcal{E}(\mathbf{k}) \tilde{\Psi}^\dagger(\mathbf{k}) U(\mathbf{k}) \beta U^\dagger(\mathbf{k}) \tilde{\Psi}(\mathbf{k}). \quad (16)$$

The quantum field nature of  $\tilde{\Psi}$  is made explicit by writing it in terms of creation and annihilation operators as follows:

$$U^\dagger(\mathbf{k}) \tilde{\Psi}(\mathbf{k}) = \begin{bmatrix} c_\uparrow(\mathbf{k}) \\ c_\downarrow(\mathbf{k}) \\ d_\uparrow^\dagger(\mathbf{k}) \\ d_\downarrow^\dagger(\mathbf{k}) \end{bmatrix} \Leftrightarrow \tilde{\Psi}(\mathbf{k}) = U(\mathbf{k}) \begin{bmatrix} c_\uparrow(\mathbf{k}) \\ c_\downarrow(\mathbf{k}) \\ d_\uparrow^\dagger(\mathbf{k}) \\ d_\downarrow^\dagger(\mathbf{k}) \end{bmatrix},$$

where  $c^\dagger(\mathbf{k})$  and  $c(\mathbf{k})$  create and annihilate bare electrons and  $d^\dagger(\mathbf{k})$  and  $d(\mathbf{k})$  create and annihilate bare positrons of definite momentum  $\hbar\mathbf{k}$ . The up- and down-arrow subscripts indicate the spin of the relevant particle. Using this notation, we arrive at the well-known form

$$H_D = \int d^3\mathbf{k} \mathcal{E}(\mathbf{k}) [c_\uparrow^\dagger(\mathbf{k})c_\uparrow(\mathbf{k}) + c_\downarrow^\dagger(\mathbf{k})c_\downarrow(\mathbf{k}) - d_\uparrow(\mathbf{k})d_\uparrow^\dagger(\mathbf{k}) - d_\downarrow(\mathbf{k})d_\downarrow^\dagger(\mathbf{k})]. \quad (17)$$

Requiring anticommutation relations, we then have

$$H_D = \int d^3\mathbf{k} \mathcal{E}(\mathbf{k}) [c_\uparrow^\dagger(\mathbf{k})c_\uparrow(\mathbf{k}) + c_\downarrow^\dagger(\mathbf{k})c_\downarrow(\mathbf{k}) + d_\uparrow^\dagger(\mathbf{k})d_\uparrow(\mathbf{k}) + d_\downarrow^\dagger(\mathbf{k})d_\downarrow(\mathbf{k}) - 2\delta(\mathbf{k} - \mathbf{k})I]. \quad (18)$$

As usual, we neglect the infinite  $\delta$  function term since it is proportional to the identity and an overall energy shift does not affect the dynamics of measurables. Equivalently, one can enforce normal ordering from the onset.

The next term in  $H_{\text{QED}}$  is the Coulomb term which describes interactions between charged particles:

$$H_C = \int d^3\mathbf{r} \int d^3\mathbf{r}' \frac{\rho(\mathbf{r})\rho(\mathbf{r}')}{8\pi\epsilon_0\|\mathbf{r} - \mathbf{r}'\|}, \quad (19)$$

with

$$\rho(\mathbf{r}) = q\Psi^\dagger(\mathbf{r})\Psi(\mathbf{r}). \quad (20)$$

The product of  $\rho$  terms in Eq. (19) results in all (normal-ordered) charge-conserving permutations of the product of four creation and annihilation operators for the various electrons and positrons. However, for the current paper, we project the  $H_{\text{QED}}$  operator onto the smallest set of occupation numbers that still allows for nontrivial scattering between matter and radiation. As we find below, this can be accomplished by retaining just two types of states: those giving rise to the measurement of exactly one (bare) electron and exactly zero photons; and those giving rise to the measurement of exactly one (bare) electron and exactly one photon. Under this projection all matrix elements between allowed states have zero contribution from the Coulomb term because the combination of four creation and annihilation operators always results in an annihilation operator killing a vacuum ket or a creation operator (acting to the left) killing a vacuum bra. This reflects

the fact that, in quantum field theory, at least two charged particles must be present for a Coulomb interaction to occur. Thus, the Coulomb term makes no contribution to the result after our one-electron projection is applied.

The third term in the QED Hamiltonian is the radiation term

$$H_R = \int d^3\mathbf{k} \hbar\omega_{\mathbf{k}} [a_1^\dagger(\mathbf{k})a_1(\mathbf{k}) + a_2^\dagger(\mathbf{k})a_2(\mathbf{k})], \quad (21)$$

where  $\omega_{\mathbf{k}} = ck$ . The creation operator  $a_j^\dagger(\mathbf{k})$  and the annihilation operator  $a_j(\mathbf{k})$  create and destroy photons with linear polarization  $\epsilon_j(\mathbf{k})$  and definite momentum  $\hbar\mathbf{k}$ .

The final term in  $H_{\text{QED}}$  is the interaction term

$$H_I = -qc \int d^3\mathbf{r} \Psi^\dagger(\mathbf{r}) [\boldsymbol{\alpha} \cdot \mathbf{A}_\perp(\mathbf{r})] \Psi(\mathbf{r}). \quad (22)$$

In three spatial dimensions the vector potential has the following second-quantized form:

$$\mathbf{A}_\perp(\mathbf{r}) = \int d^3\mathbf{k} \sum_{j=1,2} \sqrt{\frac{\hbar}{2\epsilon_0\omega_{\mathbf{k}}(2\pi)^3}} \times [a_j(\mathbf{k})\epsilon_j(\mathbf{k})e^{i\mathbf{k}\cdot\mathbf{r}} + a_j^\dagger(\mathbf{k})\epsilon_j(\mathbf{k})e^{-i\mathbf{k}\cdot\mathbf{r}}]. \quad (23)$$

Enforcing spatial periodicity in the  $x$  and  $y$  directions with arbitrary lateral dimensions  $\ell \times \ell$ , the interaction term becomes

$$H_I = -cq \left(\frac{\hbar}{2\epsilon_0 c 2\pi \ell^2}\right)^{\frac{1}{2}} \sum_{n,m,n',m'} \int dk_z \int dk_z' \hat{h}_I(\mathbf{k}', \mathbf{k}), \quad (24)$$

where

$$\mathbf{k} = \mathbf{k}_{nm} = (2\pi n/\ell, 2\pi m/\ell, k_z) \quad (25)$$

and  $n, m, n'$ , and  $m'$  take on all integer values from  $-\infty$  to  $+\infty$  in the indicated sums. The momentum-resolved energy density operator  $\hat{h}_I(\mathbf{k}', \mathbf{k})$  is

$$\hat{h}_I(\mathbf{k}', \mathbf{k}) = : \begin{bmatrix} c_\uparrow^\dagger(\mathbf{k}') \\ c_\downarrow^\dagger(\mathbf{k}') \\ d_\uparrow(\mathbf{k}') \\ d_\downarrow(\mathbf{k}') \end{bmatrix}^T U^\dagger(\mathbf{k}') \mathcal{A} U(\mathbf{k}) \begin{bmatrix} c_\uparrow(\mathbf{k}) \\ c_\downarrow(\mathbf{k}) \\ d_\uparrow^\dagger(\mathbf{k}) \\ d_\downarrow^\dagger(\mathbf{k}) \end{bmatrix} : \quad (26)$$

where the colons indicate normal ordering and

$$\mathcal{A} = \sum_{j=1,2} \frac{a_j(\mathbf{k}' - \mathbf{k})\boldsymbol{\alpha} \cdot \boldsymbol{\epsilon}_j(\mathbf{k}' - \mathbf{k}) + a_j^\dagger(\mathbf{k} - \mathbf{k}')\boldsymbol{\alpha} \cdot \boldsymbol{\epsilon}_j(\mathbf{k} - \mathbf{k}')}{\sqrt{\|\mathbf{k}' - \mathbf{k}\|}}. \quad (27)$$

Under the spatial periodicity requirement, the anticommutation and commutation relations include both Kronecker and Dirac  $\delta$  functions, for example,

$$\{c_\downarrow(\mathbf{k}'), c_\downarrow^\dagger(\mathbf{k})\} = I\delta_{n,n'}\delta_{m,m'}\delta(k'_z - k_z), \quad (28)$$

$$[a_i(\mathbf{k}'), a_j^\dagger(\mathbf{k})] = I\delta_{i,j}\delta_{n,n'}\delta_{m,m'}\delta(k'_z - k_z). \quad (29)$$

In the interest of computational tractability, we now project the full  $H_{\text{QED}}$  operator onto one preferred spatial dimension,  $z$ , in which nontrivial dynamics are allowed. In the other two spatial dimensions,  $x$  and  $y$ , we make the assumption of periodicity and project onto only the lowest (constant) mode.

This spatial projection makes all wave functions arising from the reduced theory independent of  $x$  and  $y$ . For example, a wave function that describes the probability of finding a bare electron and a photon at time  $t$  in the neighborhood of spatial coordinates  $(x_e, y_e, z_e)$  for the electron and  $(x_\gamma, y_\gamma, z_\gamma)$  for the photon, and which would therefore have been of the form  $\psi_{e\gamma}(x_e, y_e, z_e; x_\gamma, y_\gamma, z_\gamma; t)$  in the full 3D theory of QED, will now be of the simpler form  $\psi_{e\gamma}(z_e; z_\gamma; t)$ . While the suppressed dimensions  $x$  and  $y$  still exist after the projection and are necessary to describe three-dimensional concepts such as polarization and spin, there is no remaining spatial variation in those transverse dimensions after the projection.

Applying this projection, the interaction term of the QED Hamiltonian becomes

$$H_I = -cq \left( \frac{\hbar}{2\epsilon_0 c 2\pi \ell^2} \right)^{1/2} \int dk'_z \int dk_z \hat{h}_I(\mathbf{k}'_{00}, \mathbf{k}_{00}), \quad (30)$$

the radiation term becomes

$$H_R = \int dk_z \hbar \omega_{\mathbf{k}_{00}} [a_1^\dagger(\mathbf{k}_{00}) a_1(\mathbf{k}_{00}) + a_2^\dagger(\mathbf{k}_{00}) a_2(\mathbf{k}_{00})], \quad (31)$$

and the Dirac term becomes

$$H_D = \int dk_z \mathcal{E}(\mathbf{k}_{00}) [c_1^\dagger(\mathbf{k}_{00}) c_1(\mathbf{k}_{00}) + c_2^\dagger(\mathbf{k}_{00}) c_2(\mathbf{k}_{00}) + d_1^\dagger(\mathbf{k}_{00}) d_1(\mathbf{k}_{00}) + d_2^\dagger(\mathbf{k}_{00}) d_2(\mathbf{k}_{00})]. \quad (32)$$

The vector  $\mathbf{k}_{00}$  indicates a wave vector with components  $(0, 0, k_z)$  as per Eq. (25).

Even after projecting onto a preferred spatial direction, the model described by Eqs. (30)–(32) is still computationally intractable, since it allows for arbitrarily large numbers of photons and any number of charged particles. To reduce the computational space, we choose an initial state with a single electron and project onto a subspace that allows for at most one photon. This projection is given by

$$\mathcal{P} = \int dk_e \left[ c_1^\dagger(k_e \hat{\mathbf{z}}) | \rangle \langle | c_1(k_e \hat{\mathbf{z}}) + \int dk_\gamma c_2^\dagger(k_e \hat{\mathbf{z}}) a^\dagger(k_\gamma \hat{\mathbf{z}}) | \rangle \langle | a(k_\gamma \hat{\mathbf{z}}) c_2(k_e \hat{\mathbf{z}}) \right]. \quad (33)$$

In the last term in Eq. (33) we have employed photonic creation and annihilation operators without subscripts; they create or destroy right- and left-hand circularly polarized photons. This basis is more natural for describing photons in Compton scattering than the linear basis because the described photons carry definite angular momentum. Mathematically, the two circular polarizations separately give the smallest invariant subspaces in which angular momentum is well-defined, and investigation of one of the subspaces provides all the information extractable from the other. Equivalently, the spin state for the bare electron we chose to consider couples to, and only to, one of these circularly polarized photons, not both. The spin state for the bare electron that we chose not to consider would couple to, and only to, photons with the opposite circular polarization.

In terms of the linearly polarized photon creation and annihilation operators, the circularly polarized photon creation and annihilation operators are given by

$$a^\dagger(k_\gamma) := \frac{a_1^\dagger(k_\gamma \hat{\mathbf{z}}) + i \text{sign}(k_\gamma) a_2^\dagger(k_\gamma \hat{\mathbf{z}})}{\sqrt{2}}, \quad (34)$$

$$a(k_\gamma) := \frac{a_1(k_\gamma \hat{\mathbf{z}}) - i \text{sign}(k_\gamma) a_2(k_\gamma \hat{\mathbf{z}})}{\sqrt{2}}. \quad (35)$$

Note that in the projection (33) the bare electron state  $c_1^\dagger(k_e \hat{\mathbf{z}}) | \rangle$  is spin up, whereas the bare electron state in the correlated pair state  $c_2^\dagger(k_e \hat{\mathbf{z}}) a^\dagger(k_\gamma \hat{\mathbf{z}}) | \rangle$  is spin down. This is important because if we keep the spins the same, for each linear polarization  $j$  we have

$$\begin{aligned} & \langle a_j(k_\gamma \hat{\mathbf{z}}) c_\uparrow(k_e \hat{\mathbf{z}}) | H_I c_\uparrow^\dagger(k_z \hat{\mathbf{z}}) | \rangle \\ & \propto \frac{\delta(k_z - k_e - k_\gamma)}{|k_\gamma|^{1/2}} [U^\dagger(k_e \hat{\mathbf{z}}) \boldsymbol{\alpha} \cdot \boldsymbol{\epsilon}_j(k_\gamma \hat{\mathbf{z}}) U(k_z \hat{\mathbf{z}})]_{1,1} \\ & = 0, \end{aligned} \quad (36)$$

where the subscripts on the bracketed  $4 \times 4$  matrix give the row and column indices. On the other hand, one finds that for the opposite output spin we get the nontrivial results

$$\begin{aligned} & \langle | a_j(k_\gamma \hat{\mathbf{z}}) c_\downarrow(k_e \hat{\mathbf{z}}) | H_I c_\uparrow^\dagger(k_z \hat{\mathbf{z}}) | \rangle \\ & \propto \frac{\delta(k_z - k_e - k_\gamma)}{|k_\gamma|^{1/2}} [U^\dagger(k_e \hat{\mathbf{z}}) \boldsymbol{\alpha} \cdot \boldsymbol{\epsilon}_j(k_\gamma \hat{\mathbf{z}}) U(k_z \hat{\mathbf{z}})]_{2,1}, \end{aligned} \quad (37)$$

where

$$\begin{aligned} & [U^\dagger(k_e \hat{\mathbf{z}}) \boldsymbol{\alpha} \cdot \boldsymbol{\epsilon}_j(k_\gamma \hat{\mathbf{z}}) U(k_z \hat{\mathbf{z}})]_{2,1} = [i\delta_{j1} - \text{sign}(k_\gamma)\delta_{j2}] \\ & \times i \left[ S \left( \frac{\hbar k_e}{mc} \right) C \left( \frac{\hbar k_z}{mc} \right) - S \left( \frac{\hbar k_z}{mc} \right) C \left( \frac{\hbar k_e}{mc} \right) \right]. \end{aligned} \quad (38)$$

The first term in Eq. (38) demonstrates the appropriateness of the circular polarization basis described in Eqs. (34) and (35). The terms  $C$  and  $S$  are defined by

$$\begin{aligned} C(p) &= \sqrt{\frac{1}{2} \left( 1 + \frac{1}{h_e(p)} \right)}, \\ S(p) &= \text{sign}(p) \sqrt{\frac{1}{2} \left( 1 - \frac{1}{h_e(p)} \right)}, \end{aligned} \quad (39)$$

with

$$h_e(p) = \sqrt{1 + p^2}, \quad (40)$$

Here we have defined the unitless momentum  $p$  as  $p = \hbar k/mc$ .

The projection (33) allows us to study a much simpler model comprised of a single electron and at most one photon described by a unitless reduced Hamiltonian  $\mathcal{H}$  given by

$$\mathcal{H} = \frac{1}{mc^2} \mathcal{P} H_{\text{QED}} \mathcal{P} = \mathcal{H}_e + \mathcal{H}_\gamma + \mathcal{H}_{e,\gamma}. \quad (41)$$

With this projection, the Schrödinger equation (3) can be written in a unitless form,

$$i \frac{\partial}{\partial \tau} |\psi\rangle = \mathcal{H} |\psi\rangle, \quad (42)$$

where  $\tau = tmc^2/\hbar$ . We define unitless state basis vectors as follows:

$$|p_e\rangle = \sqrt{\frac{mc}{\hbar}} c_{\uparrow}^{\dagger} \left( \frac{mcp_e}{\hbar} \hat{\mathbf{z}} \right) | \rangle, \quad (43)$$

$$|p_e, p_{\gamma}\rangle = \frac{mc}{\hbar} c_{\downarrow}^{\dagger} \left( \frac{mcp_e}{\hbar} \hat{\mathbf{z}} \right) a^{\dagger} \left( \frac{mcp_{\gamma}}{\hbar} \hat{\mathbf{z}} \right) | \rangle. \quad (44)$$

With these unitless vectors, we can then write the reduced Hamiltonian terms as

$$\mathcal{H}_e = \int dp_e h_e(p_e) \left( |p_e\rangle \langle p_e| + \int dp_{\gamma} |p_e, p_{\gamma}\rangle \langle p_e, p_{\gamma}| \right),$$

$$\mathcal{H}_{\gamma} = \int dp_e \int dp_{\gamma} h_{\gamma}(p_{\gamma}) |p_e, p_{\gamma}\rangle \langle p_e, p_{\gamma}|,$$

$$\mathcal{H}_{e,\gamma} = \int dp_e \int dp'_e g(p'_e, p_e) (|p'_e, p_e - p'_e\rangle \langle p_e| + \text{H.c.}), \quad (45)$$

where

$$h_{\gamma}(p) = |p|, \quad (46)$$

$$g(p', p) = \eta \frac{S(p')C(p) - S(p)C(p')}{\sqrt{|p - p'|}},$$

and  $\eta$  is the coupling strength between matter and radiation, defined by

$$\eta = \frac{\hbar}{m_e c \ell} \sqrt{\alpha}, \quad (47)$$

where  $\alpha$  is the fine-structure constant.

Note that the denominator in the coupling  $g(p', p)$  goes to zero when the input momentum  $p$  and the output momentum  $p'$  of the electron are the same, which corresponds to no change in the electron's momentum whence the photon's momentum being zero. Fortunately, the numerator in  $g$  goes to zero faster than the denominator in this case, so that  $g(p, p) = 0$  and the cross section for "scattering" with no actual change in the fermion's momentum is zero. We emphasize that this fortunate structure is encoded in full 3D QED and that our projection down onto a single nontrivial space dimension does not lose this benign feature. The exact details of this structure are those needed in the minimal coupling approach to preserve the Lorentz covariance of the theory.

### III. COMPTON SCATTERING

We can use this reduced Hamiltonian to model Compton scattering under this simplifying projection. To do this, we choose an initial state  $|\psi_0\rangle$  as a tensor product state such that the electron and photon portions are individually Gaussian. These distributions are, respectively, centered at positions  $x_{0e}$  and  $x_{0\gamma}$ , with spatial widths  $w_e$  and  $w_{\gamma}$ , and central momenta  $p_{0e}$  and  $p_{0\gamma}$ , so that

$$|\psi_0\rangle = \int dp_e \int dp_{\gamma} \psi(p_e, p_{\gamma}) |p_e, p_{\gamma}\rangle, \quad (48)$$

where

$$\psi(p_e, p_{\gamma}) = \phi(p_e - p_{0e}, w_e, x_{0e}) \phi(p_{\gamma} - p_{0\gamma}, w_{\gamma}, x_{0\gamma}) \quad (49)$$

and

$$\phi(p, w, x) = \sqrt{\frac{w}{\sqrt{2\pi}}} \exp \left[ -\frac{p^2 w^2}{4} - ipx \right]. \quad (50)$$

The unitless scaled position  $x$  is related to the physical position  $X$  by  $x = X m_e c / \hbar$ . The electron portion of this initial state is not a fully dressed electron. Such a dressed initial state would require more photons than are in this simplified system, both to dress the electron and to scatter from it. Nevertheless, the initial state (48) gives the proper projection of the more complicated initial state (dressed with additional photons) onto the states available in our reduced system.

Importantly this projection onto our current state space does not yield a state with any bare electron component in it. This might seem strange at first if one only briefly considers that a dressed electron in this model is such a bare electron state superposed with correlated electron-photon pairs. However, it becomes immediately understandable once one considers that what we want here is the tensor product of such a dressed state with yet another photon: one gets the described correlated electron-photon pairs that we use here, and, in addition, gets states with a bare electron correlated with two photons, and a bare electron never arises in any such superposition.

To model dynamics, we discretize the unitless momentum  $p$  and use a finite number of the corresponding discretized momentum states to create a matrix representation of the reduced Hamiltonian  $\mathcal{H}$  in momentum space. In our previous paper [11], we discuss in detail the considerations needed when choosing a discretization grid. We then spectrally resolve the matrix representation to find the states of well-defined energy within this discretized model which have straightforward dynamics, and then we use these states to generate the time propagator for the Schrödinger equation as usual. With this propagator in hand, we can choose an initial state and compute its time-resolved evolution.

To compute Compton scattering, we choose an initial state with the electron located at  $x_{0e} = 0.94\hbar/m_e c$  and the photon located at  $x_{0\gamma} = -0.94\hbar/m_e c$ , with equal spatial widths  $w_e = w_{\gamma} = 0.25\hbar/m_e c$  and opposite central momenta  $p_{0e} = -0.03m_e c$  and  $p_{0\gamma} = 0.03m_e c$ . We use a coupling of  $\eta = 0.4$ , which corresponds to a transverse discretization length scale of  $\ell \approx 0.1$  pm. Figure 1 plots the evolution of the joint probability distribution  $|\psi(p_e, p_{\gamma})|^2$  for these parameters as time progresses. At early times, the joint probability distribution resembles the initial condition with electron and photon momenta centered on their initial values. During the scattering process, the probability shifts into the scattered states with opposite momenta.

To visualize the evolution of this initial state in the spatial domain, we compute the Fourier transform of the joint probability amplitude

$$\psi(x_e, x_{\gamma}) = \frac{1}{2\pi} \int dp_e \int dp_{\gamma} \psi(p_e, p_{\gamma}) e^{ip_e x_e} e^{ip_{\gamma} x_{\gamma}}. \quad (51)$$

The evolution of  $|\psi(x_e, x_{\gamma})|^2$  is shown for various times in Fig. 2, where the dashed line represents the collection of points where the electron and photon positions are the same. The scattering is spatially local, as can be seen by noting that scattering does not occur until the distribution crosses



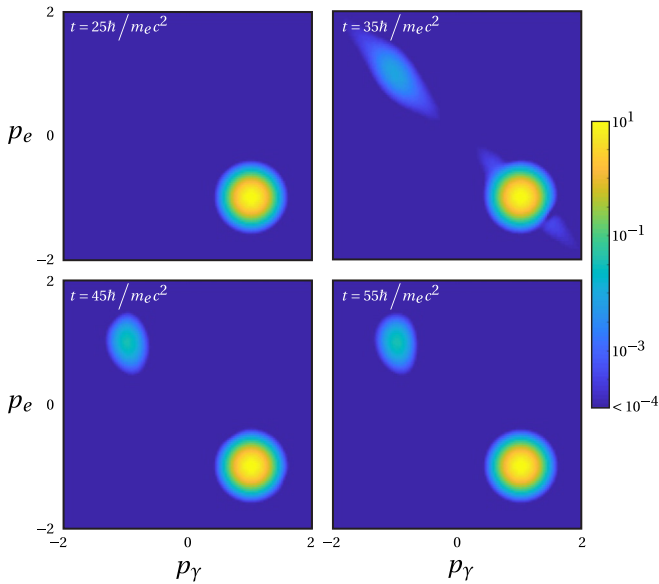


FIG. 1. Time evolution of the joint probability distribution  $|\psi(p_e, p_\gamma)|^2$  as time progresses for the initial state described in the text.

this equal-position line where the electron and photon states spatially overlap.

As the system evolves, the vertical (electron) component of the joint probability distribution spreads while the horizontal (photon) component does not, resulting in a vertically elongated joint probability distribution for the unscattered portion of the state. Thus, during the scattering process, the narrower photon scatters over a wider range of spatial locations where the electron probability is present, resulting in the scattered portion of the distribution being horizontally elongated. Since the electron is spreading throughout the interaction, the scattered portion of the distribution at large times is asymmetric.

Note the interference of the unscattered and the scattered portions of the distribution at  $t = 40\hbar/m_e c^2$  when these two portions overlap. We see evidence of this spatial interference in the  $S$ -matrix results below, albeit only in momentum space. Presumably this is because  $S$ -matrix theory only yields, for any given initial data to be propagated by the full propagator for the interacting theory, the corresponding initial data to be evolved freely that nevertheless gives the same asymptotic dynamics. Thus to visualize the spatial interference evident at early times during the full propagation, it appears that evolving freely the effective data that  $S$ -matrix theory yields is crucial, here turning the interference phenomena evident only in momentum space (for the  $S$ -matrix results) into the corresponding interference phenomenon evident only in physical space and only at early times in the full dynamics.

We emphasize that Figs. 1 and 2 illustrate the scattering dynamics of a fully second-quantized theory, projected down to one dimension. The model represents an electron moving and interacting with the photon in a self-consistent way. The scattering dynamics evident in these plots, including the electron spreading and the interference, are distinctively quantum mechanical features which are only indirectly available in the corresponding  $S$ -matrix theory. Below, we show evidence that in  $S$ -matrix theory one seems to need to propagate (freely) the

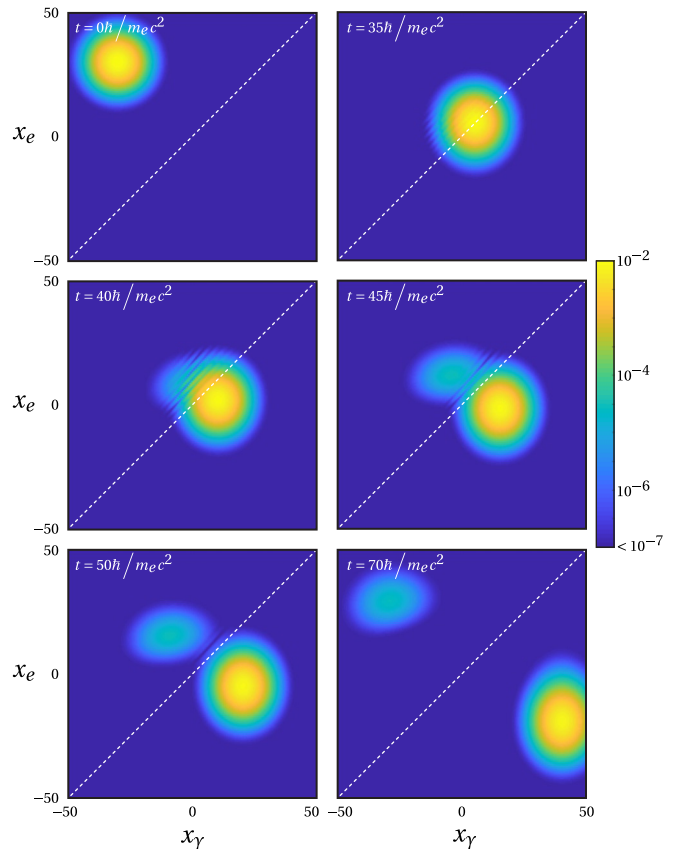


FIG. 2. Time evolution of the joint probability distribution  $|\psi(x_e, x_\gamma)|^2$ , the Fourier transform of the distribution plotted in Fig. 1.

effective, scattered data it generates in order for interference phenomena encoded in momentum space to show itself as the corresponding interference phenomena noticed at early times in physical space under the full evolution.

#### IV. COMPARISON TO THE $S$ -MATRIX APPROACH

We now compare the fully time-resolved results above to the standard second-order scattering theory. The usual development of that theory involves, roughly speaking, comparing a state  $|\psi_{-\infty}\rangle$  evolved from  $t = -\infty$  to time  $t = 0$  with a co-state  $\langle\psi_{+\infty}|$  evolved from  $t = +\infty$  back to time  $t = 0$ , while necessarily removing the effects of free evolution of the bare particles to get convergence. Therefore, the scattering operator is often defined by considering the product of Møller wave operators, essentially given by

$$\hat{S} = \left( \lim_{t \rightarrow \infty} e^{it\mathcal{H}} e^{-it\mathcal{H}_0} \right)^\dagger \lim_{t \rightarrow \infty} e^{-it\mathcal{H}} e^{it\mathcal{H}_0}, \quad (52)$$

where  $\mathcal{H}_0 = \mathcal{H}_e + \mathcal{H}_\gamma$  [3].

$S$ -matrix theory provides a mathematical map between data to be evolved according to the full propagator and effective data to be evolved freely, the correspondence made by demanding the long-time dynamics be asymptotically the same. In the Møller wave operator approach the  $S$  operator is the composition of two maps. The first map is from the *final* data for the free problem to actual final data for the full one (each

to be evolved backwards in time, whence “final”). The second map is from the actual initial data for the full problem onto equivalent effective initial data for the free problem (each to be evolved forwards in time, whence “initial”). Then one thinks of what is here the intermediate actual data for the full problem as both the relevant final and relevant initial data. Because of this precise definition, the following issues arise: does the first map from the effective final data to the actual final data exist? Less loosely, on what subspace of the Hilbert space does it exist? And for that map one wonders whether, even when it exists (i.e., on which subspace), it will map onto the actual initial data for the full problem we would like to consider. The latter is the matter of asymptotic completeness. Note that the latter issue arises because we consider the inverses of what might be reasonably considered the more natural mappings: One could argue that it is more natural to directly try to develop a map from the actual (initial or final) data (to be evolved fully) to the corresponding effective data to be evolved freely. We use this idea in order to circumvent the issue of completeness and replace it with only a consideration of existence, as follows.

Instead of thinking of the first map suggested in Eq. (52) as acting on data for the free problem, we think of it as acting on data intended for the full problem. It should be the case that the distinction can be made as small as one likes by making sure the data for the full problem includes only particles well-separated whence not interacting. Here we do this by making sure that in our time-resolved dynamics of the full problem no interactions appear to occur until well into the evolution when the particles start to spatially overlap. Thus there is an

important test suggested here, namely that our model allows the particles to be asymptotically free, i.e., that our model is purely spatially local. Given the way we derived our model, there is no guarantee of this *a priori*—we have thrown away antimatter, which is mathematically crucial to getting perfect spatial locality. However, the nonlocality that our model must necessarily exhibit seems to be made arbitrarily small in effect as the interaction is made weak. In practice, we have never observed particles interacting before their spatial wave functions overlap in our numerical simulations.

With the initial data swapped in this way, the only remaining issue is that of existence, for both maps indicated in Eq. (52), the second of which (the one on the left) actually being the inverse of the operator suggested in the Möller wave operator approach (which we have not described here fully). For the latter the issue of asymptotic completeness arises because we hope that the indicated Hermitian conjugate is the same as the suggested inverse, meaning defined on a large enough space to include states that we want to scatter. If these maps exist, the first with data swapped so that it acts on only initial data of the full problem, the overall map arising from their composition does too, and one might hope that that composition is directly computable: We find it is, exactly so.

In the Appendix we show that if one defines the  $\hat{S}$  operator more directly via

$$\hat{S} = \lim_{t \rightarrow \infty} e^{i\mathcal{H}t_0} e^{-2i\mathcal{H}t} e^{i\mathcal{H}t_0}, \quad (53)$$

its matrix elements can be computed explicitly, without any perturbative approximation, assuming the operator exists on the relevant subspace of our Hilbert space. The result is

$$\langle p'_\gamma, p'_e | \hat{S} - I | p_e, p_\gamma \rangle = -2\pi i \delta(E(p'_e, p'_\gamma) - E(p_e, p_\gamma)) \frac{\delta(p'_e + p'_\gamma - p_e - p_\gamma) g(p'_e + p'_\gamma, p'_e) g(p_e + p_\gamma, p_e)}{E(p_e, p_\gamma) - E(p'_e + p'_\gamma) + i\epsilon + \int dp \frac{g(p_e + p_\gamma, p_e + p_\gamma - p)^2}{E(p_e + p_\gamma - p, p) - E(p_e, p_\gamma) - i\epsilon}}, \quad (54)$$

where  $I$  is the identity operator, the energy of a bare electron state is

$$E(p_e) = h_e(p_e), \quad (55)$$

the bare energy of an electron-photon state is

$$E(p_e, p_\gamma) = h_e(p_e) + h_\gamma(p_\gamma), \quad (56)$$

and  $\epsilon$  is a positive infinitesimal. To second order in perturbation theory, Eq. (54) gives

$$\begin{aligned} \langle p'_\gamma, p'_e | \hat{S}^{(2)} | p_e, p_\gamma \rangle &= \frac{-2i\pi \delta(E(p'_e, p'_\gamma) - E(p_e, p_\gamma))}{E(p_e, p_\gamma) - E(p'_e + p'_\gamma) + i\epsilon} \\ &\times \delta(p'_e + p'_\gamma - p_e - p_\gamma) \\ &\times g(p'_e + p'_\gamma, p'_e) g(p_e + p_\gamma, p_e). \end{aligned} \quad (57)$$

The first  $\delta$  function in Eq. (54) describes conservation of energy, and the second  $\delta$  function describes conservation of momentum. The perturbative approximation described above makes errors on the order of  $\eta^3$  in general, but for terms such as Eq. (54), which are traditionally used to describe Compton scattering, the error is on the order of  $\eta^4$ , as can be seen by comparison with the exact formula. Importantly, this version of  $\hat{S}$  agrees to the indicated order with that obtained by the

standard time-dependent perturbation theory, truncating the relevant Neumann series at second order.

Applying the here-developed version of  $\hat{S}$  to the specific initial state used to create Figs. 1 and 2, we have

$$|\psi_{+\infty}\rangle = \hat{S} |\psi_{-\infty}\rangle = \hat{S} |\psi_0\rangle. \quad (58)$$

Note here our mapping of the effective initial data for the free system (to be propagated backwards in time in the Möller operator approach) to the actual initial data of the full problem. Again, this assumes that our model allows, at least approximately, for our particles to be asymptotically free. Using the second-order perturbation representation of  $\hat{S}$  allows us to calculate the projection of the output state  $|\psi_{+\infty}\rangle$  onto the pair states as

$$\psi^{(2)}(p_e, p_\gamma) = \langle p_e, p_\gamma | \psi_{+\infty} \rangle. \quad (59)$$

Figure 3 plots  $\psi^{(2)}$  compared to the initial data. Figure 3(a) shows the initial spatial distribution and Fig. 3(b) plots the initial momentum distribution. After applying the scattering theory above, we plot the scattered spatial distribution  $|\psi^{(2)}(x_e, x_\gamma)|^2$  in Fig. 3(c) and the corresponding momentum distribution  $|\psi^{(2)}(p_e, p_\gamma)|^2$  in Fig. 3(d). The scattering theory distribution plotted in Fig. 3 agrees with the overall

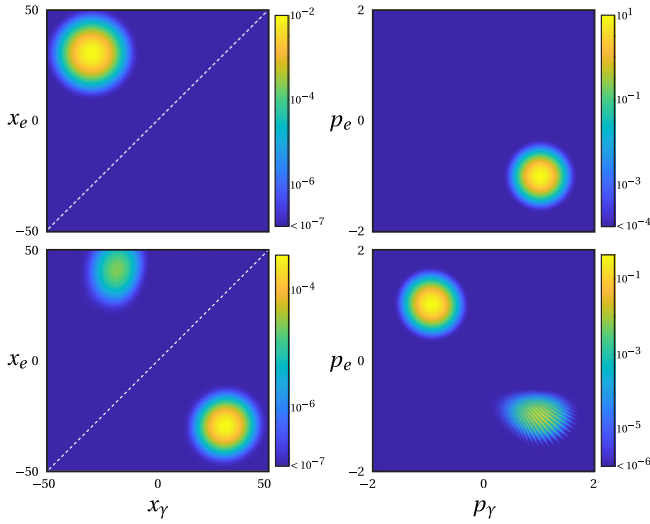


FIG. 3. (a) The initial spatial distribution  $|\psi(x_e, x_\gamma)|^2$  as in Fig. 2. (b) The initial momentum distribution  $|\psi(p_e, p_\gamma)|^2$  as in Fig. 1. (c) The scattered joint probability in space distribution  $|\psi^{(2)}(x_e, x_\gamma)|^2$ . (d) The scattered joint probability distribution in momentum  $|\psi^{(2)}(p_e, p_\gamma)|^2$ .

magnitude of scattering shown in our time-resolved plots in Fig. 1. Recall that all frames of Fig. 3 represent data at the initial time; the latter two frames represent the effective data to be propagated freely. Figures 3(a) and 3(b) propagate forward with interactions to eventually arrive at a condition where all further dynamical interactions appear finished and further propagation is asymptotically free. Figures 3(c) and 3(d) represent initial conditions that, if propagated freely at all times (i.e., with no interaction, but only the trivial standard quantum spreading effects), would result eventually in the very same dynamics as for the previous case in the long-time limit. Presumably the structure evident in the momentum plot in Fig. 3(d) encodes the interference and dynamical behavior discussed above in relation to the spatial version of the full dynamics animations.

## V. CONCLUSION

It might be somewhat surprising that we can, in a qualitatively correct way, model electron-photon scattering with such few photons. Previous work regarding the minimal dressing of bare electrons to become full-fledged electrons required dressing of a bare electron with at least one photon. This allows the dressed object to acquire spatial stability, meaning that the dressed object's spatial structure becomes time invariant aside from the usual quantum spreading. So, *a priori*, it might not have been surprising to have learned that one needed multiple photons to describe the process: at least one to dress the electron and another to scatter.

Various ways of misthinking this scenario exist. In addition to the error described previously, another possible misinterpretation would be to think that to observe Compton scattering one needs to start with a bare electron and a spatially separated single photon, expecting the bare electron to dress itself locally with the photon in addition to scattering from the sepa-

rated portion of that same photon. This is incorrect for several reasons, mainly the misinterpretation of correlated states as not being the same as tensor product states. For example, one must realize that this other photon is necessarily correlated to another electron in the charge-1 subspace, so that this would not be the scenario of pure Compton scattering, but rather would include the scattering of two electrons as well. Alternatively, if it is actually a pure photon state, not correlated with an additional electron, because of charge conservation, the evolution of the latter exists in another invariant subspace of our Hilbert space, and any overall wave function describing the two separated subspaces simply describes the usual Schrödinger cat superposition of the two kinds of uncorrelated states.

To better understand why the simplified system in this paper does not allow the electron to locally dress itself before scattering, as suggested earlier, consider a state with a dressed electron, denoted by  $|e\rangle_d$ , correlated with an additional “scattered” photon state, denoted by  $|\gamma'\rangle$ . We can write this sort of tensor product state in the form

$$\begin{aligned} |e\rangle_d |\gamma'\rangle &= \left( \mathcal{C}(e)|e\rangle_b + \sum_\gamma \mathcal{C}(e, \gamma)|e_\gamma\rangle_b |\gamma\rangle \right) |\gamma'\rangle \\ &= \mathcal{C}(e)|e\rangle_b |\gamma'\rangle + \sum_\gamma \mathcal{C}(e, \gamma)|e_\gamma\rangle_b |\gamma\rangle |\gamma'\rangle, \end{aligned} \quad (60)$$

where  $\mathcal{C}$  represents the probability amplitudes for the various basis states. Note that the final form of this state contains three-particle states which are outside the scope of the simplified system. Projecting Eq. (60) back onto states with no more than one photon as in this paper, we find

$$\begin{aligned} P_{0,1\gamma}|e\rangle_d |\gamma'\rangle &= P_{0,1\gamma} \left( \mathcal{C}(e)|e\rangle_b |\gamma'\rangle + \sum_\gamma \mathcal{C}(e, \gamma)|e_\gamma\rangle_b |\gamma\rangle |\gamma'\rangle \right) \\ &= \mathcal{C}(e)P_{0,1\gamma}|e\rangle_b |\gamma'\rangle + \sum_\gamma \mathcal{C}(e, \gamma)P_{0,1\gamma}|e_\gamma\rangle_b |\gamma\rangle |\gamma'\rangle \\ &= \mathcal{C}(e) \cdot 1|e\rangle_b |\gamma'\rangle + \sum_\gamma \mathcal{C}(e, \gamma)0|e_\gamma\rangle_b |\gamma\rangle |\gamma'\rangle \\ &= \mathcal{C}(e)|e\rangle_b |\gamma'\rangle, \end{aligned} \quad (61)$$

that is,

$$P_{0,1\gamma}|e\rangle_d |\gamma'\rangle = \mathcal{C}(e)|e\rangle_b |\gamma'\rangle. \quad (62)$$

Thus, in our minimal model with no “extra” scattering photon, we encode the initial data of a dressed electron correlated with a scattering photon onto just the bare correlated pair states  $|e\rangle_b |\gamma'\rangle$ . This mapping makes an error on the order of the size of the vector of dressing coefficient values  $\mathcal{C}(e, \gamma)$ , which becomes arbitrarily small for arbitrarily small couplings between radiation and matter. This observation is consistent with standard *S*-matrix theory where one typically considers scattering between bare particle states and not dressed states.

The time-resolved approach described above yields results comparable to standard scattering theory and provides a more direct access to the time-resolved dynamics of the interaction. Moreover, to observe these same dynamical



effects in scattering theory, one must first calculate the scattered “initial data” and then use free propagation to observe the ensuing dynamics. We have found that, at least for the specific problem studied here, analyzing dynamics directly using the approach introduced in this work is computationally less demanding than generating even the analogous information from scattering theory. Our method directly produces visualizations of the scattering process in both space and momentum representations. While we have restricted to the case of an electron-photon interaction here, this time-resolved approach can be extended to the study of electron-electron interactions and to include multiple dimensions. For electron-electron interactions, the Coulomb term will become important in the second-quantized Hamiltonian.

### ACKNOWLEDGMENTS

This work is supported by the National Science Foundation under Grant No. 1708185.

### APPENDIX

When it exists, we can compute the matrix elements of  $\hat{S}$  defined in Eq. (53) exactly because of three facts. The first fact is that, when this limit exists, it is the same as that which is given by the “Abel limit”:

$$\begin{aligned} \hat{S} &\equiv \left( A - \lim_{t \rightarrow \infty} \right) e^{+itH_0} e^{-2itH} e^{+itH_0} \\ &\equiv \lim_{\epsilon \downarrow 0} \int_0^\infty dt \epsilon e^{-\epsilon t} e^{+itH_0} e^{-2itH} e^{+itH_0}. \end{aligned} \quad (\text{A1})$$

The second fact is that for any self-adjoint operator  $H$ , and for any time  $t > 0$ , we have the following spectral resolutions:

$$\begin{aligned} \exp(-itH) &= \lim_{\epsilon \downarrow 0} \frac{1}{-2\pi i} \int d\lambda \frac{e^{-i\lambda t}}{\lambda + i\epsilon - H}, \\ \exp(itH) &= \lim_{\epsilon \downarrow 0} \frac{1}{2\pi i} \int d\lambda \frac{e^{i\lambda t}}{\lambda - i\epsilon - H}. \end{aligned} \quad (\text{A2})$$

Inserting Eq. (A2) into the right-hand side of Eq. (A1), accomplishing the time integral, and then taking matrix elements with respect to eigenstates of  $H_0$ , represented by  $\langle \beta |$  and  $|\alpha\rangle$ , gives a triple integral over the  $\lambda$  spectral variables that can be accomplished using Cauchy’s theorem. The result of this triple integration is

$$\begin{aligned} &\langle \beta | \left( A - \lim_{t \rightarrow \infty} \right) e^{+itH_0} e^{-2itH} e^{+itH_0} |\alpha\rangle \\ &= \lim_{\epsilon \downarrow 0} \langle \beta | \frac{i\epsilon}{\frac{E_0(\beta) + E_0(\alpha)}{2} + i\epsilon - H} |\alpha\rangle, \end{aligned} \quad (\text{A3})$$

where  $E_0(\alpha)$  gives the eigenvalue for  $|\alpha\rangle$  and likewise for the state  $\langle \beta |$ . This result is completely general, applicable to many problems in addition to the one studied here.

The last fact is that the operator between  $\langle \beta |$  and  $|\alpha\rangle$  in Eq. (A3) is a resolvent for  $H$  and for the particular model considered in this paper, can be derived exactly. For Compton scattering, we are interested in  $|\alpha\rangle = |p, q\rangle$  and  $\langle \beta | = \langle p', q'|$ , and one finds that

$$\begin{aligned} \frac{1}{z - H} |p, q\rangle &= \frac{|p, q\rangle}{z - E_0(p, q)} \\ &+ \frac{\frac{g(p+q, p)}{z - E_0(p, q)}}{z - E_0(p+q) + \int d\tilde{p}_\gamma \frac{g(p+q, p+q-\tilde{p}_\gamma)^2}{E_0(p+q-\tilde{p}_\gamma, \tilde{p}_\gamma) - z}} \\ &\times \left( |p+q\rangle + \int dp_\gamma \frac{g(p+q, p+q-p_\gamma)}{z - E_0(p+q-p_\gamma, p_\gamma)} \right) \\ &\times |p+q-p_\gamma, p_\gamma\rangle \end{aligned} \quad (\text{A4})$$

Inserting Eq. (A4) into Eq. (A3), using  $z = [E(p', q') + E(p, q)]/2 + i\epsilon$ , and taking the limit  $\epsilon \rightarrow 0$  gives the result in Eq. (54).

- 
- [1] I. Sigal, *Scattering Theory for Many-Body Quantum Mechanical Systems* (Springer, Berlin, 1983).
- [2] M. E. Peskin and D. V. Schroeder, *An Introduction to Quantum Field Theory* (Westview, Boca Raton, FL, 1995).
- [3] E. Zeidler, *Quantum Field Theory II: Quantum Electrodynamics* (Springer-Verlag, Berlin, 2009).
- [4] D. Krebs, D. A. Reis, and R. Santra, Time-dependent QED approach to x-ray nonlinear Compton scattering, *Phys. Rev. A* **99**, 022120 (2019).
- [5] M. Fuchs, M. Trigo, J. Chen, S. Ghimire, S. Shwartz, M. Kozina, M. Jiang, T. Henighan, G. N. C. Bray, P. H. Bucksbaum, Y. Feng, S. Herrmann, G. A. Carini, J. Pines, P. Hart, C. Kenney, S. Guillet, S. Boutet, G. J. Williams, M. Messerschmidt *et al.*, Anomalous nonlinear x-ray Compton scattering, *Nat. Phys.* **11**, 964 (2015).
- [6] S. Norris, J. Unger, Q. Z. Lv, Q. Su, and R. Grobe, Removal of self-interactions in the Dirac-Maxwell equations in one spatial dimension, *Phys. Rev. A* **93**, 032131 (2016).
- [7] T. Cheng, E. R. Gospodarczyk, Q. Su, and R. Grobe, Numerical studies of a model fermion-boson system, *Ann. Phys.* **325**, 265 (2010).
- [8] R. E. Wagner, Q. Su, and R. Grobe, Time-resolved Compton scattering for a model fermion-boson system, *Phys. Rev. A* **82**, 022719 (2010).
- [9] R. E. Wagner, M. R. Ware, B. T. Shields, Q. Su, and R. Grobe, Space-Time Resolved Approach for Interacting Quantum Field Theories, *Phys. Rev. Lett.* **106**, 023601 (2011).
- [10] R. E. Wagner, M. R. Ware, Q. Su, and R. Grobe, Space-time properties of a boson-dressed fermion for the Yukawa model, *Phys. Rev. A* **82**, 032108 (2010).
- [11] S. Glasgow, D. Smith, L. Pritchett, J. Gardiner, and M. J. Ware, Space-time-resolved quantum electrodynamics: A (1+1)-dimensional model, *Phys. Rev. A* **93**, 062106 (2016).
- [12] C. Cohen-Tannoudji, J. Dupont-Roc, and G. Grynberg, *Photons and Atoms: Introduction to Quantum Electrodynamics* (Wiley, New York, 2007).